On a Drag Coefficient of Solid Cylindrical Capsule

On a Drag Coefficient of Solid Cylindrical Capsule*

by

Katsuya YANAIDA and Shoichiro FUJISAWA**

(Received September 5, 1975)

Summary

In this paper the authors deal with the solid cylindrical capsule which are falling through transparent and vertical tube filled with water.

A capsule drag coefficient is determined by measuring the terminal velocity of small scale models in this case.

It is clear from the results of this investigation that in spite of fundamental differences in flow around falling capsule and freely-suspended capsule drag coefficients are approximately the same for practical purposes in both cases.

1. Introduction

The problem of capsule transport has been studied by many reserchers, but important subject on the basic factor in a capsule-pipe system has been left solved.

Lazarus and Kilner[1] discussed the incipient motion of solid capsule in pipe-lines without considering on the drag coefficient of capsule, whereas Carstens[2] or Hammit[3] determined the drag coefficient of capsule under the only blockage conditions.

The flow field chracteristics and drag of spheres had been a classical problem requring both theoretical and experimental work[4] for many years. However, we noted that Round, Latto and Anzenavs[5] dealt in the main with the drag coefficient associated with freely-suspended trains of rigidly attached spheres in water and that the results of their were in very good agreement with the experimental that of McNown and Newlin[6] in the case of flow pattern past stationary spheres.

As indicated above, similar approaches were executed. However, in general these included additional simplifications, such as neglecting the capsule wall shear in the vicinity of the tube.

In this paper such a subject is pointed out ant is discussed hydrodynamically a drag coefficient of freely-suspended and falling solid cylindrical capsule in a vertical tube with water as the working fluid.

Experimenting with falling solid cylindrical capsule through vertical tube filled with water, the authors presented experimental results and correlations and noted the effect of capsule/pipe diameter ratio, capsule length/diameter ratio and capsule specific gravity on the drag coefficient of capsule.

It may be interested in this paper that there is a tendancy for the data of falling solid cylindrical capsule of the current investigation to lie above the characteristic curved line on a drag coefficient of freely-suspended solid cylindrical capsule obtained in the previous report.[7]

Nomenclature

B buoyant force

C_{ds} coefficient of drag based on hindered settling capsule surface area

---

* Held at University of Kobe, Organised by JSME of Kansai (1975–11)

** Department of Mechanical Engineering

C_{df} coefficient of drag based on freely-suspended capsule surface area
$\bar{d}$ diameter ratio, d/D
D tube diameter
d capsule diameter
F shear force
g acceleration due to gravity
K diameter ratio, D/d
l capsule length
$\bar{l}$ capsule length/diameter ratin, l/d
P pressure
P_0 pressure at section (0)
P_1 pressure at section (1)
P_2 pressure at section (2)
Q volumetric flow rate
r radius coordinate
R_e annulus Reynolds number relative to capsule
U fluid velocity in tube relative to capsule
U_s terminal settling velocity of capsule
U_{fm} superficial mean velocity of freely-suspended capsule
U_{sm} superficial mean velocity of hindered settling capsule
W weight of capsule
Z axial coorcinate
α axial pressure gradient term, $\frac{1}{4\mu}\frac{dp}{dz}\cdot r^2$
Γ dimensionless shear coefficient
κ dimensionless pressure coefficient
μ viscosity of fluid
ν kinematic viscosity of fluid
ξ $(1-\bar{d}^2)^2$
ρ density of fluid
$\bar{\rho}_c$ capsule density ratio
τ_c shear stress on capsule

2. General Analysis and Correlations

In the present paper a one-dimensionnal fully established annular flow analysis is doveloped and compared with the experimental results for various factors of capsule. Further, the fully developed annulus flow result is then applied as the basis for correlation of the experimental data.

Fig. 1 depicts a flow pattern around the hindered settling capsule. In this section, the velocity and shear stress distribution in the annulus and fluid dynamic drag coefficients are calculated.

To solve this problem, the flow is assumed to be one-dimensional, steady, laminar by a constant property, single phase, incompressible, Newtonian fluid through concentric annulus between a capsule and a longer cylindrecal tube.

Considering these assumptions the Navier- Stokes equations for the fluid motion in the annulus simplify to

$$\frac{dp}{dz}=\mu\left[\frac{1}{r}\frac{d}{dr}\left(r\cdot\frac{du}{dr}\right)\right] \tag{1}$$

The boundary conditions for coordinates fixed on the capsule are:

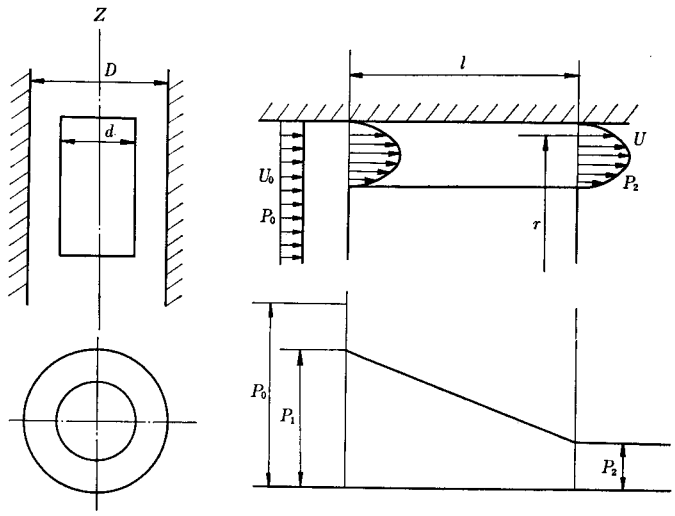

Fig. 1 Flow Patterns around the hindered Settling Capsule.

$$U = 0 \quad \text{at} \quad r = \frac{D}{2} \tag{2}$$

$$U = 0 \quad \text{at} \quad r = \frac{d}{2} \tag{3}$$

Intergartion of Eq. (1) and incorporation of the two boundary conditions yields

$$U(r) = -\alpha\left[\frac{1}{r^2}\left(\frac{d}{2}\right)^2 - 1 + \frac{\left\{\left(\frac{D}{2}\right)^2 - \left(\frac{d}{2}\right)^2\right\}}{r^2 \ln K} \ln \frac{r}{\left(\frac{d}{2}\right)}\right] \tag{4}$$

where

$$\alpha = \frac{1}{4\mu} \cdot \frac{dP}{dZ} r^2, \quad K = \frac{D}{d}$$

The rate of volumetric flow displaced by a falling capsule is

$$Q = \int_0^{2\pi} \int_{d/2}^{D/2} U r dr d\theta = -\frac{\pi}{8\mu} \frac{dP}{dZ}\left[\left(\frac{D}{2}\right)^4 - \left(\frac{d}{2}\right)^4 - \frac{\left\{\left(\frac{D}{2}\right)^2 - \left(\frac{d}{2}\right)^2\right\}^2}{\ln K}\right] \tag{5}$$

From Eq. (5), the average velocity through the annulus can now be related to the hindered settling velocity by applying the continuity equation between cross sections with and without the capsule:

$$Q = \frac{\pi}{4} d^2 U_s \tag{6}$$

$$U_{sm} = \frac{Q}{\frac{\pi}{4}(D^2 - d^2)} \tag{7}$$

$$= \frac{U_s}{K^2 - 1} \tag{8}$$

Conbination of Eq. (5), Eq. (7) and Eq. (8) yields a relation between annulus pressure drop and average velocity through the annulus and hindered settling velocity of capsule:

$$U_{sm} = -\frac{\left(\frac{d}{2}\right)^2}{8\mu}\frac{dP}{dZ}\left[(K^2+1)-\frac{K^2-1}{\ln K}\right] \tag{9}$$

$$U_s = -\frac{\left(\frac{d}{2}\right)^2}{8\mu}\frac{dP}{dZ}(K^2-1)\left[(K^2+1)-\frac{K^2-1}{\ln K}\right] \tag{10}$$

The drag force on the cylindrical capsule can now be calculated by applying a force balance to the capsule:

$$W-B = (P_0-P_2)\frac{\pi}{4}d^2+\int_0^l \tau_c \pi d dx \tag{11}$$

Then, we define a drag coefficient of falling capsule as follows:

$$C_{ds} = \frac{W-B}{\frac{\rho}{2}U_{sm}^2\cdot\frac{\pi}{4}d^2} \tag{12}$$

The dimensionless shear coefficient results in Eq. (13)

$$\Gamma = \frac{\int_0^l \tau_c \pi d dx}{\frac{\rho}{2}U_{sm}^2\cdot\frac{\pi}{4}d^2} = -\frac{F\cdot l}{\frac{\rho}{2}U_{sm}^2\cdot\frac{\pi}{4}d^2} \tag{13}$$

where

$$F = -2\pi\mu\left(\frac{d}{2}\right)\left[\frac{dU}{dr}\right]_{r=d/2}$$

and differentiating Eq. (4) with respect to r, we obtain

$$\frac{dU}{dr} = -\alpha\left[-\frac{2}{r}+\frac{\left\{\left(\frac{D}{2}\right)^2-\left(\frac{d}{2}\right)^2\right\}}{r^3\ln K}\right] \tag{14}$$

then

$$\Gamma = \frac{64\bar{l}}{\left[(K^2+1)-\frac{K^2-1}{\ln K}\right]R_e}\left[\frac{K^2-1}{2\ln K}-1\right] \tag{15}$$

where

$$R_e = \frac{U_{sm}d}{\nu}$$

The dimensionless pressure coefficient is determined from Eq. (9) and application of Bernoulli's mechanical energy equation between section 0 and 1 and between section 1 and 2:

$$\kappa = \frac{P_0-P_2}{\frac{\rho}{2}U_{sm}^2} = \frac{P_0-P_1}{\frac{\rho}{2}U_{sm}^2}+\frac{P_1-P_2}{\frac{\rho}{2}U_{sm}^2} \tag{16}$$

$$= (1-\xi)+\frac{64\bar{l}}{\left[(K^2+1)-\frac{K^2-1}{\ln K}\right]R_e} \tag{17}$$

The wetted area drag coefficient may be obained from Eq. (15) and Eq. (17). It is

$$C_{ds} = \Gamma + \kappa$$
$$= (1-\xi) + \frac{64\bar{l}}{\left[(K^2+1) - \frac{K^2-1}{\ln K}\right] R_e} \cdot \left[\frac{K^2-1}{2 \ln K}\right] \tag{18}$$

Thus, the wetted area drag coefficient is of the from

$$C_{ds} = f(K, \bar{l}, R_e) \tag{19}$$

3. Experimental Investigation

In order to the coplexity of the physical situation in the near flow field when a capsule travels through a tube, the major emphasis of this investigation has been placed on experimentation.

The experiments have been dealt with scale models and cylindrical tube; taking advantage of the principle of dynamical similitude which permits the results to be applied to full scale capsules and tubes that satisfy the similitude requirements.

Since a wide range of geometric parameters are investigated, the drag coefficient must be considered a function of the capsule and tube geometry in addition to the capsule Reynolds number.

3.1 Apparatus and Experimental Procedure

The experimental apparatus can be descrived with the aid of a schmatic diagram Fig. 2. The apparatus consists of three main elements; pipe-lining, the models and the instrumentation.

(1) Pipe-lining

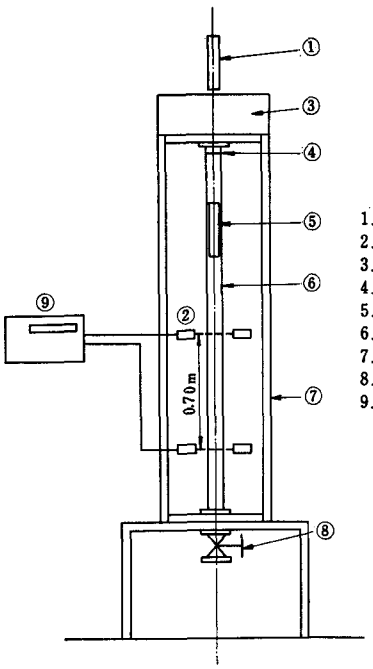

1. Capsule model
2. Photo cells
3. Injection tank
4. Fluid level
5. Falling model
6. Transparent acylic plastic tube
7. Supporting frame
8. Drain valve
9. Amplifier and stop clock

Fig. 2 Experimental Apparatus

Table, 1

material	specific gravity	capsule dia mm	capsule length/dia ratio $\bar{l}$	relative roughness k/d	inner dia & relative roughbess
lucite	1.15	41.0	1.5 2.0 2.5 3.0 3.5 4.0 5.0 6.0	0.104×10^{-3}	acrylic pipe $D=50.0$ mm $K/D=0.022\times0^{-3}$
		45.0	1.5 2.0 2.5 3.0 4.0	0.094×10^{-3}	
		47.7	1.5 2.0 2.5 3.0 4.0 4.5	0.089×10^{-3}	
	1.19	41.3	1.5 2.0 2.5 3.5 4.0 6.0	0.034×10^{-3}	
		45.3	1.5 2.0 2.5 3.0 4.0 4.7	0.031×10^{-3}	
	1.41	41.0	1.5 2.0 2.5 3.0 3.5 4.0 6.0	0.021×10^{-3}	
		43.4	1.5 2.0 3.0 3.5 4.0 5.0	0.046×10^{-3}	
		46.0	1.5 2.5 3.0 3.5 4.0 5.0	0.043×10^{-3}	
		47.7	1.5 2.0 2.5 3.0 3.5 5.0	0.042×10^{-3}	
aluminum	2.70	45.0	1.5 2.0 2.5 3.0 4.0 5.0	0.267×10^{-3}	
		47.0	1.5 2.0 2.5 3.0	0.255×10^{-3}	
		48.0	1.5 2.0 3.0 4.0	0.250×10^{-3}	
steel (freely-suspended)	7.80	45.0	1.5 2.0 3.0 4.0	0.104×10^{-3}	
		47.0	1.5 2.0	0.100×10^{-3}	
		48.0	1.5 2.0 3.0	0.098×10^{-3}	

The vertical pipe line was supported by a structural frame fabricated from prepunched structural components. The frame was fixed to the concrete floor.

The data from which the correlation were developed were taken in transparent acrylic pipe 2 m. length and 0.05m. in diameter. Sufficient length was provided between the capsule injection point and the test section to eliminate entrance effects before any measurement were made.

(2) Models

The models are depicted in Fig. 2 with their geometric and dynamic chacteristics listed in table 1. The models consisted of a flat-ended cylindrical solid capsules.

(3) Instrumentation

The terminal velocity of the capsule can be determined by measuring its time of travel between the two phototransducers using a digital counter reading to one millisecond.

(4) Procedure

The experimental procedure was straight forward. The procedure used to determine the drag coefficient was to measure the terminal velocity during a falling capsule in vertical pipe with water under the influence gravity. Capsule were injected singly, and on passing the first photocell. This arrangement allowed the mean capsule terminal velocity over the 2m. length test section to be calculated.

3.2 Results and Discussion

3.2.1 Average Velocity Through the Annulus, U_{sm}

We may be able to obtain the average velocity through the annulus as defined in Eq. (8) by means of measuring the terminal velocity of capsule. The effect on the velocity of each of capsule factors will now be discussed. The curves which are defined the annular flow analysis and the boundary layer theoretical portions are shown as solid lines and as dash-dot lines respectively in figures.

(1) The effect of diameter ratio, $\bar{d}$

The velocity decreases with increasing diameter ratio at variable capsule length and at constant capsule density in Fig. 3.

The results obtained from measurements for $\bar{d}$ can be compared with those of analyses in

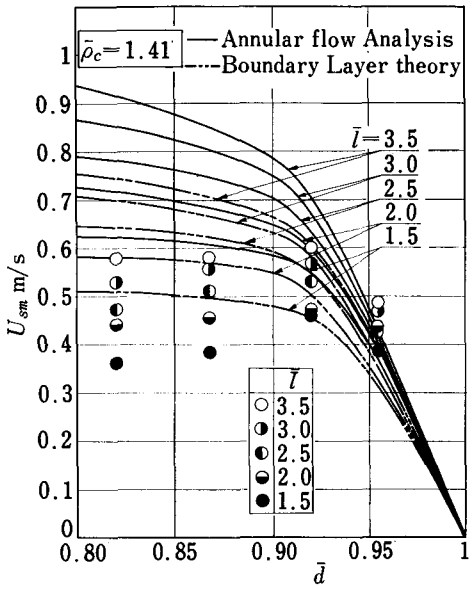

Fig. 3 Variation of U_{sm} with $\bar{d}$ and $\bar{l}$ for $\bar{\rho}_c$=1.41

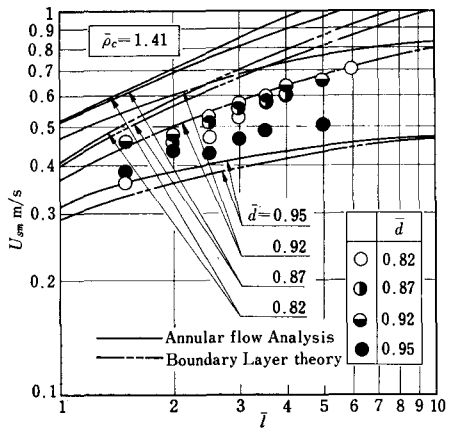

Fig. 4 Variation of U_{sm} with $\bar{l}$ and $\bar{d}$ for $\bar{\rho}_c$=1.41

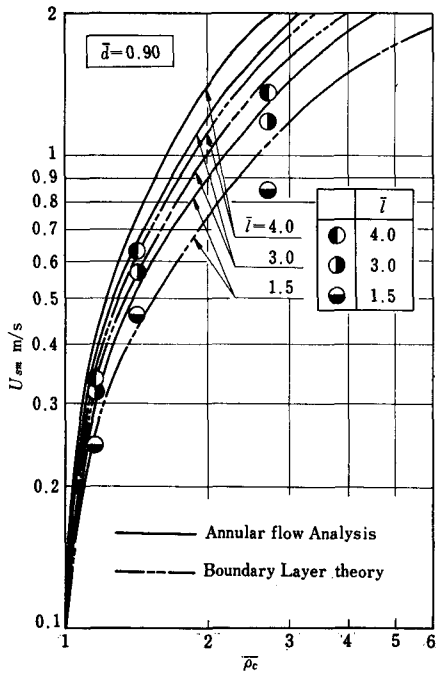

Fig. 5 Variation of U_{sm} with $\bar{l}$ and $\bar{\rho}_c$ for $\bar{d}$=0.90

Fig. 3. Considerable scatter is evident, the results presumably depending upon the method of experimentation, the stability and pitching, capsule eccentricity and the capsule rotation. Also shown in Fig. 3 is a solid curve line representing theoretical value which is seen to coincide rather closely with the experimental result for $\bar{d}$ equal to 0.96. Theoretical analysis can thus be used in the extraporation of these results to still larger values of $\bar{d}$.

(2) The effect of capsule length/diameter ratio, $\bar{l}$

The velocity increases with increasing length/diameter ratio, and the effect increases as capsule diameter decreases. In Fig. 4, the velocity is plotted against $\bar{l}$ with $\bar{d}$ as a parameter for a constant capsule density. It is apparent from this figure that a solid curve line for annular flow analysis is seen to conincide rather closely with the experimental result for $\bar{d}$ equal to 0.95.

(3) The effect of capsule density ratio, $\bar{\rho}_c$

Fig. 5 depicts the velocity versus with $\bar{l}$ as a parameter for a constant $\bar{d}$ equal to 0.90. The effect of increasing capsule density, other factors being constant, is to increase the velocity.

Then, the effect of density ratio is much larger, and higher threshold water velocities are needed before the capsule will move.

3.2.2 Wetted area drag coefficient, C_{ds}

The experimental wetted area drag coefficient is obtained from the equation (12). The variations in wetted area drag coefficient caused by changes of diameter ratio $\bar{d}$, length/diameter ratio $\bar{l}$ and capsule density ratio will now be discussed.

(1) The effect of diameter ratio, $\bar{d}$

Fig. 6 shows C_{ds} versus $\bar{d}$ with $\bar{l}$ as a parameter for a constant capsule density ratio $\bar{\rho}_c$ equal to 1.15. From Fig. 6, it is apparent that the experimental data deviate very sharply from the theoretical curve lines at the smaller diameter ratio of capsule, but for larger values of $\bar{d}$ the experimental data coincide rather closely with the theoretical values.

(2) The effect of capsule length/diameter ratio, $\bar{l}$

Fig. 7 depicts C_{ds} against $\bar{l}$ with $\bar{d}$ as a parameter for a conatant capsule density ratio $\bar{\rho}_c$ equal to 2.70.

It is apparent drom this figure that C_{ds} does not become independent of capsule length ratio, $\bar{l}$ for values of $\bar{d}<0.90$.

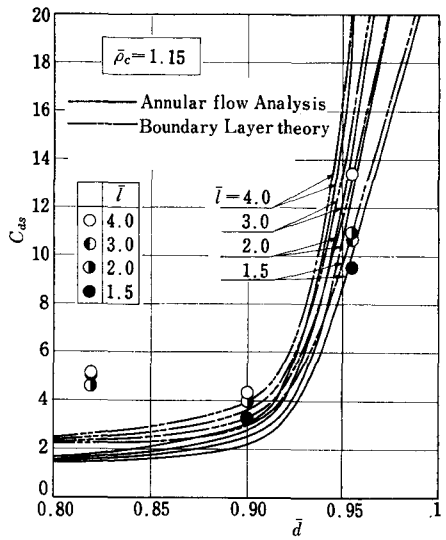

Fig. 6 Variation of C_{ds} with $\bar{d}$ and $\bar{l}$ for $\bar{\rho}_c$=1.15

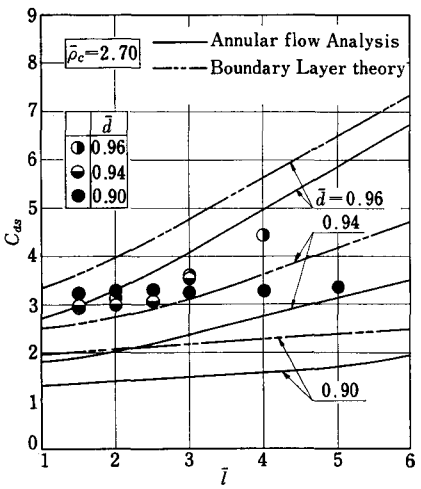

Fig. 7 Variation of C_{ds} with $\bar{l}$ and $\bar{d}$ $\bar{\rho}_c$=2.70

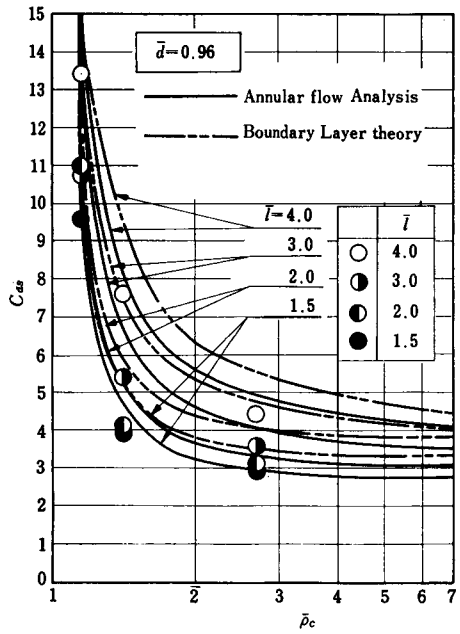

Fig. 8 Variation of C_{ds} with $\bar{l}$ and $\bar{\rho}_c$ for $\bar{d}$=0.96

However, the experimental data agree barely with the theoretical experssion of Eq. (18) for value of $\bar{d}$ equal to 0.96.

(3) The effect of capsule density ratio, $\bar{\rho}_c$

In Fig. 8, the drag coefficient is plotted against $\bar{\rho}_c$ with $\bar{l}$ as a parameter for a constant $\bar{d}$ equal to 0.96.

From this figure, it can be seen that the experimental data agree fairly well with the annular flow analytical equation (18) for value of $\bar{d}$ equal to 0.96.

3.2.3 Comparison of terminal and suspended velocity of capsule, U_{fm}/U_{sm}

The ratio suspended velocity/terminal velocity (velocity ratio) is a function of three independent variables, Viz: capsule length/diameter ratio, capsule density ratio and diameter ratio.

The effect on the velocity ratio of each of these variables as indicated by the experimental results will now be discussed.

(1) The effect of capsule length/diameter ratio, $\bar{l}$

In Fig. 9, velocity ratio is plotted against $\bar{l}$ with $\bar{d}$ as a parameter for a constant capsule density ratio $\bar{\rho}_c$ equal to 1.41.

It is apparaent from this figure that velocity ratio U_{fm}/U_{sm} becomes independent of capsule length ratio $\bar{l}$. However, as $\bar{d}$ decreases experimental data are noticeably scattered.

(2) The effect of capsule density ratio, $\bar{\rho}_c$

Fig. 10 shows U_{fm}/U_{sm} versus $\bar{\rho}_c$ with $\bar{l}$ as a parameter for diameter ratio $\bar{d}$ equal to 0.90. From this figure, it can be seen that velocity ratio becomes nearly independent of capsule density ratio.

(3) The effect diameter ratio, $\bar{d}$

Fig. 11 depicts U_{fm}/U_{sm} against $\bar{d}$ with $\bar{l}$ as a parameter for capsule density ratio $\bar{\rho}_c$ equal to 1.41. Superimposed on the experimental results of this investigation in fig. 11 are the experimental results obtained by Okuda[8] for spherical models.

It is interesting to note that the velocity ratio of cylindrical capsule for values of $\bar{d}<0.90$ may be identical with that of spherical models for values of $0.1<\bar{d}<0.4$.

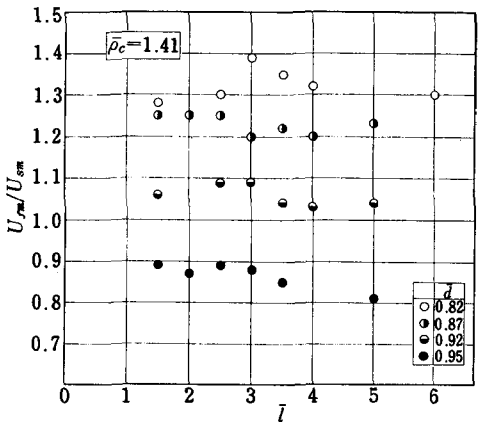

Fig. 9 The variation of velocity ratio with $\bar{l}$ and $\bar{d}$ for $\bar{\rho}_c$ 1.41

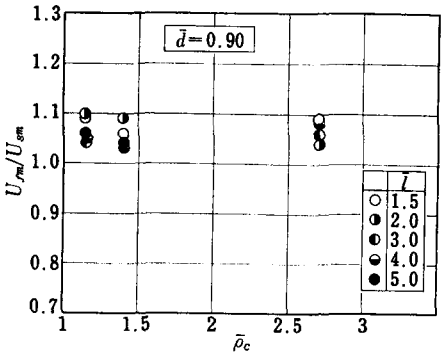

Fig. 10 The variation of velocity ratio with $\bar{\rho}_c$ and $\bar{l}$ for $\bar{d}$=0.90

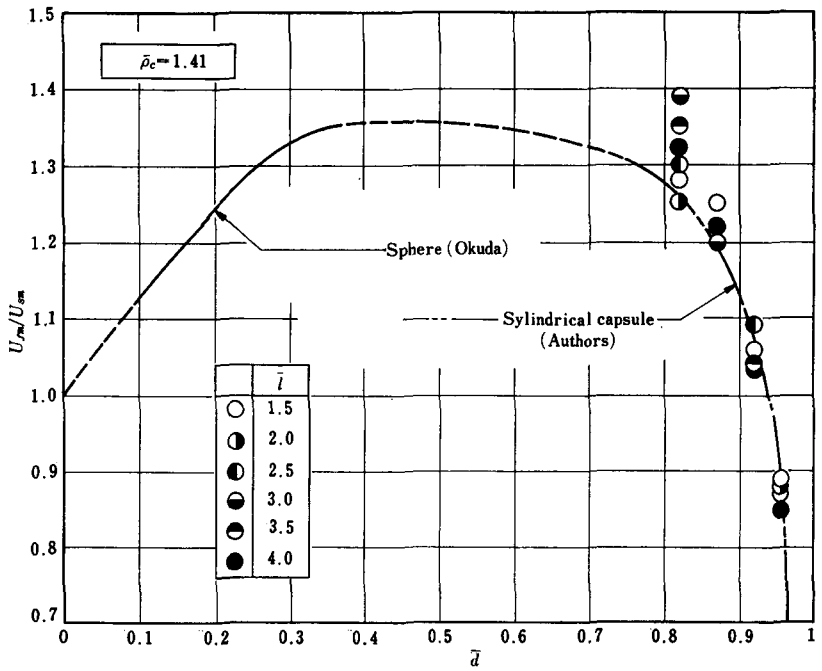

Fig. 11 Comparison of other experimental results with that of authors.

3.2.4 Characteristics of drag coefficient

The drag coefficient resulting from Eq. (18) is plotted in Fig. 12 as a function of characteristics number $\bar{l}/(1/\bar{d}-1)^2R_e$ with $\bar{d}$ as a parameter.

Also shown in Fig. 12 are the dash-pot curve lines representing the equation obtained from the hydrodynamic analysis on laminar boundary layers around a solid capsule and an inner wall of tube.

From this figure, it is interesting to note that the wetted area drag coefficient can be identical at the range of characteristics number for practical purposes in both cases which are the

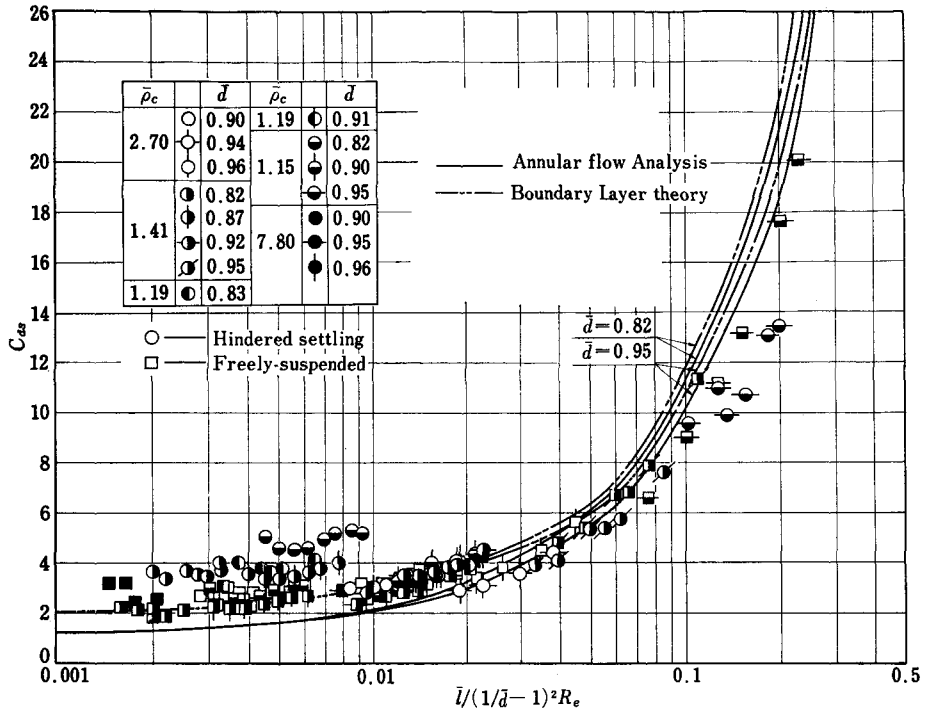

Fig. 12 Variation of C_{ds} with characteristic number with $\bar{d}$.

hindered settling and freely-suspended cylindrical capsule in a vertical tube with water. However, at the large values of characteristics number the analytic model of annular flow may be applicable for the only hindered settling capsule. From Fig. 12, it is also apparent that the effect of diameter ratio on the drag coefficient of capsule at the range of small chacteristics number is especially large for annular flow analytical model.

4. Conclusions

In this paper a drag coefficient of hindered settling capsule in a vertical tube with water is treated.

It is possible to draw the following conclusions:

1) A method of approximate caluculation of annular flow through around the hindered settling capsule is presented with a view to contributing some to design and analyzing chacteristics of the hydraulic capsule transportation.
2) The relation between a drag coefficient of hindered settling capsule and chacteristics number is clarified analytically.
3) The results show that the effect of diameter ratio is very significant for a drag coefficient of capsule.
4) The analytical values give good agreement with experimental results for $\bar{d}$ equal to 0.96 with other capsule factors.
5) A drag coefficient characteristics curve obtained from equation (18) is applicable for characteristics number $0.02<\bar{l}/(1/\bar{d}-1)^2R_e<0.08$.

Acknowledgements

The authors wish to express their gratitude to Professor Toshio Kawashima of Tohoku University and Professor Eitaro Sugino of Osaka prefectural technical college for their encouragement to the present research.

References

1) Lazarus, J.H. and Kilner, F.A. "Incipient Motion of Solid Capsules in Pipelines". Paper C3 Proceedings Hydrotransport 1, BHRA, 1970.
2) Carstens, M.R. "Analysis of a Low-Speed Capsule-Transport Pipeline". Paper C4 Proceedings Hydrotransport 1, BHRA, 1970.
3) Hammitt, A.G. "Aerodynamic Analysis of Tube Vehicle Systems". AIAA JOURNAL, 10–3, 1972.
4) Soo, S.L. "Fluid Dynamics of Multiphase Systems". Blaisdell Publishing. Comp, 1967.
5) Round, G.F., Latto, B. and Anzenavs, R. "Drag Coefficients of Freely-Suspended Spheres and Spheres Trains in a Vertical Tube". Paper F1 Proceedings Hydrotransport 2, BHRA, 1972.
6) McNown, J.S. and Newlin, J.T. "Drag of Spheres within Cylindrical Boundaries". Proc. lst. U.S. Natl. Congress Appl. Mech. Chicago, pp. 801-806, 1951.
7) Yanaida, K. and Fujisawa, S. "On the Pipeline of Capsules". Bull. Osaka Prefec. Tech. College, 8, 1974.
8) Okuda, N. "Effect of the Tube Wall on the Flow around spherical Model suspended and hindered Settling in a Tube". J. JSME, 41–342 (1975-2).